

---

## Responses of single-layer spherical reticulated shell with initial geometrical defects under multi-directional ground motions

Yahong Luo, Hongtao Zuo, Jun Gong\*, Yongbo Shao  
School of Civil Engineering and Geomatics, Southwest Petroleum University, Chengdu 610500, China  
\* jun.gong@swpu.edu.cn

### Abstract

Multi-dimensional ground motions can introduce substantial uncertainties regarding their incident direction on structures, which is unfavorable to the seismic design of structures. Generally, the ideal and centrosymmetric structure, e.g., single-layer spherical reticulated shell (SSRS), will not be threatened by the incident directionality. Yet, the seismic safety of SRSS with initial geometrical defects (IGDs) will not be ensured when ignoring the incident directionality in the design. In this study, the effect of incident directionality on responses of SSRS with IGDs (e.g., L/1000, L/700, L/500, and L/300) is numerically investigated. Seven groups of multi-dimensional ground motions are selected to excite SSRS-IGD. The multi-dimensional and multi-directional seismic excitation method is used in the nonlinear time history analysis. Seismic responses (including displacement, acceleration and reaction force), damage states and bearing capacity of SSRS-IGD in different incident directions are compared, and the distribution of critical incident angle is discussed. Different grid partition patterns and half-span loading are considered. The effects of incident directionality on responses of SRSSs with different IGDs are generated to provide reference for seismic design of SRSSs.

**Keywords:** single-layer spherical reticulated shells, initial geometrical defects, incident directionality, numerical calculation, nonlinear time history analysis, structural responses.

### 1. Introduction

The single-layer spherical reticulated shell (SSRS) is a prevalent type of long-span space structure used in large public buildings such as convention centers, shopping malls, and cultural facilities. This structure is highly valued for its light self-weight, superior spatial utilization, distinctive visual aesthetics, and extended service life. The SSRS design effectively disperses loads, ensuring good structural stability and seismic resistance. In the event of disasters like earthquakes, it maintains structural integrity, providing safe shelters for the public. Therefore, the destruction of these structures under strong earthquakes can result in significant economic losses and high numbers of fatalities. To date, several practical examples of SSRS have sustained severe damage or even total collapse during seismic events, potentially due to the anisotropic feature of seismic loading.

In recent years, numerous scholars have concentrated on the impact of the incident direction on the seismic response of structures [1], yet there is scant research available on the incident direction on SRSSs. The existing research literature primarily focuses on three main structures: buildings, bridges, and special structures. For building structures, Liang et al. [2] reached the conclusion that the impact of the seismic incident angle on the torsional response of masonry structures is very pronounced through a shaking table test. Bugueño et al. [3] also identified the significant effect of incident angle on the seismic response of reinforced concrete structures, which cannot be overlooked. Sun et al. [4] investigated the influence of the incident direction on the grid structure, and defined the main directions of time history and response spectrum. Moreover, Alam et al. [5] discovered that structures with eccentric stiffness are highly sensitive to changes in the incident direction. For bridge structures, Torbol and Shinozuka [6] and Feng et al. [7] argued that disregarding the direction of incidence could result in an underestimate

of the fragility of bridge components. For special structures, Gong et al. [8] thoroughly examined the effect of incident directionality of UHV substation structures under earthquakes.

SSRS is a complex spatial force system, and its vibration modes are spatial deformation forms, which is very different from the abovementioned buildings, bridges, and masonry structures. The effect of incident directionality on SSRS is not clear yet. This study selects a typical Kewitt SSRS as the research object. Its finite element model is established in the software ABAQUS. Then, the multidimensional and multi-directional seismic excitation method is used in the nonlinear time history analysis of SSRS. The seismic responses of SSRS with initial geometrical defects (IGDs) excited by different ground motions with multiple directions are studied. The results of this study can provide a reference for the seismic design of SSRSs.

## 2. Finite element model of SSRS

A detailed numerical model of a Kewitt typical SSRS with a rise-span ratio ( $f$ ) of  $1/3$  is modeled in the software ABAQUS. The SSRS has a span ( $L$ ) of 60m and the distributed roof load of 1.2 kN/m, which includes  $1.0 \times$  dead load ( $0.95 \text{ kN/m}^2$ ) and  $0.5 \times$  snow load ( $0.5 \text{ kN/m}^2$ ). The SSRS is supported using pinned joints at the outermost ring. The lowest order vibration mode of the SSRS is used to calculate the IGD with a defect amplitude of  $L/1000$  (0.06 m),  $L/700$  (0.0857 m),  $L/500$  (0.12 m), and  $L/300$  (0.2 m). Two mainly used sectional dimensions of steel tubes are  $152 \text{ mm} \times 5.5 \text{ mm}$  and  $146 \text{ mm} \times 5 \text{ mm}$ . The geometry of SSRS is shown in Figure 1.

A cumulative damage steel constitutive model [9] is used in the numerical model. It has a yield strength  $f_y$  of 270 MPa and Young's modulus  $E$  of  $2.1 \times 10^5 \text{ MPa}$ . The Rayleigh damping is calculated for the nonlinear dynamic analysis, using the eigenfrequencies of the first and third modes of vibration and the damping ratio is 2%.

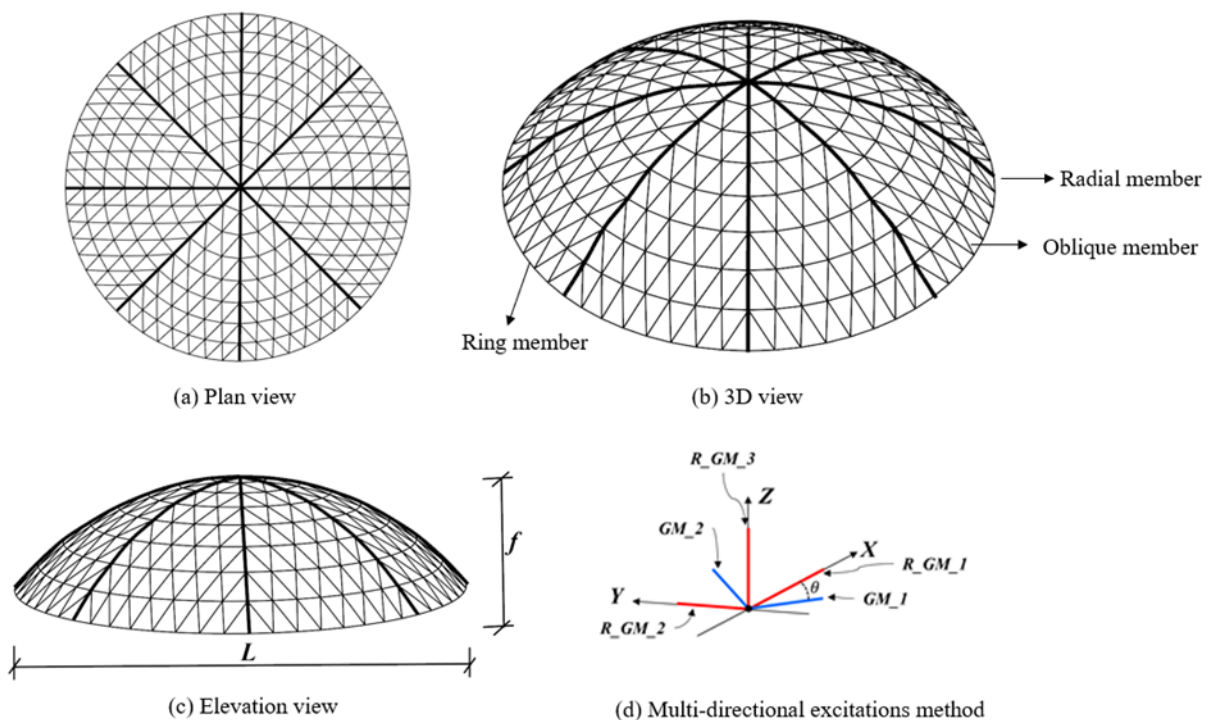


Figure 1 Multi-directional excitations on SSRS with IGDs

## 3. Ground motion selection

Seven groups of far-field ground motions are selected from NGA WEST 2 database [10], as listed in Table 1. Each group of ground motions contains three orthogonal components and satisfies the following criteria: shear wave velocity range [260,510] in m/s, magnitude interval ( $M$ ) (5.8,7.8) and epicentral

distance interval (EpiD) (20,100) in km. As shown in Figure 1(d), the two horizontal components are transformed according to Eq. (1) [11], in which the incident angle changes from  $0^\circ$  to  $360^\circ$  with an interval of  $15^\circ$ . At the same time, the vertical component does not change. After the transformation, the three components along the  $X$ ,  $Y$ , and  $Z$  directions are generated to excite the SSRS.

$$\begin{pmatrix} R_{GM_1}(t) \\ R_{GM_2}(t) \\ R_{GM_3}(t) \end{pmatrix} = \begin{bmatrix} \cos \theta & \sin \theta & 0 \\ -\sin \theta & \cos \theta & 0 \\ 0 & 0 & 1 \end{bmatrix} \begin{pmatrix} GM_1(t) \\ GM_2(t) \\ GM_3(t) \end{pmatrix} \quad (1)$$

where  $\theta$  denotes the angle of seismic incidence;  $GM_1(t)$ ,  $GM_2(t)$ , and  $GM_3(t)$  denote the three recorded components;  $R_{GM_1}(t)$ ,  $R_{GM_2}(t)$ , and  $R_{GM_3}(t)$  denote the rotated components; and  $t$  is time.

Table 1: Seven selected ground motions.

NGA No.	Name	$M$	EpiD(km)	Year
0030	Parkfield	6.19	32.56	1966
0138	Tabas, Iran	7.35	74.66	1978
0308	Taiwan SMART1(5)	5.9	30.5	1981
0816	Georgia, USSR	6.2	72.39	1991
0907	Big Bear-01	6.46	49.42	1992
0945	Northridge-01	6.69	52.89	1994
1181	Chi-Chi, Taiwan	7.62	71.63	1999

The engineering site of the shell structure has a classification of II with a peak ground acceleration (PGA) of 0.2 g. To study the influence of incident direction on structural responses subjected to earthquakes with different intensities, the frequently occurring earthquakes (FOEs), design-based earthquakes (DBEs), maximum considered earthquakes (MCEs), and extremely rare earthquakes (EREs) are used to excite the SSRS. Their PGAs are 0.07, 0.20, 0.40, and 0.60 g, respectively.

## 4. Results and discussion

The characteristic of SSRS is that its stability and carrying capacity are significantly affected by vertical deformation. Therefore, the vertical displacement of the nodes, the vertical acceleration of the nodes and the stress of the members are selected as engineering demand parameters (EDPs), and the changes under different incident angles are analyzed, so as to determine the influence of the incident direction on the seismic response of SSRS. Percentile values ( $Rotnn$ ) (i.e.,  $Rot00$ ,  $Rot100$ , and  $Rot50$ ) are used to quantify the directional seismic responses of SCRS.  $Rot00$ ,  $Rot100$ , and  $Rot50$  represent the minimum, maximum, and median values respectively of seismic response among all ASIs.  $Rot100/Rot00$  is defined to characterize the maximum difference of quantities caused by the incident direction.

### 4.1 Response of SSRS with different IGDs

Under the excitation of ground motion NGA0945, Figure 2 indicates that the maximum vertical displacement of the structure varies with the incident angle, displaying a periodic pattern around three main angles. Under the condition of a higher earthquake magnitude (0.4g) and larger initial defect of  $L/300$ , the vertical displacement at the incident angle of  $15^\circ$  is 0.0763 m. When compared with 0.0735 m at  $30^\circ$ , they have a minor difference of only 6.5%. Similarly, the maximum vertical acceleration does not vary significantly with the incident angle, as shown in Figure 3. The response reaches its highest value of 21.46 m/s<sup>2</sup> at  $0^\circ$  and dips slightly to 20.06 m/s<sup>2</sup> at  $15^\circ$ , with a minimal variation of 7.0%. Additionally, the maximum stress distribution shown in Figure 4 is examined. A stress level of 321.3 MPa is observed at  $30^\circ$  and that is 314.3 MPa at  $0^\circ$ , indicating a small difference of 2.2%.

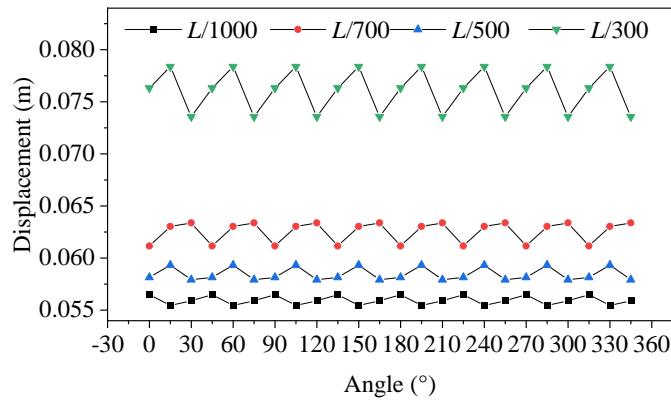


Figure 2: Maximum displacement of SSRS-IGD.

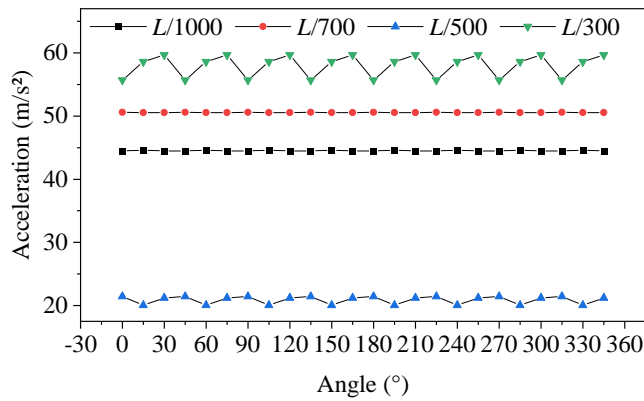


Figure 3: Maximum acceleration of SSRS-IGD.

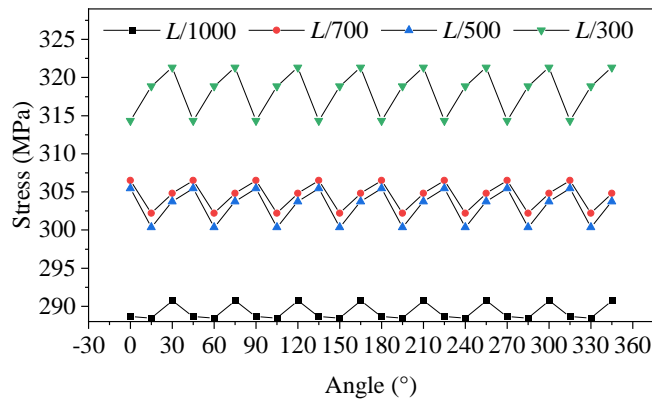


Figure 4: Maximum stress of SSRS-IGD.

When the SSRS-IGD is subjected to seven seismic excitations, the maximum value of  $Rot_{100}/Rot_{00}$  of the vertical displacement changing with the incident direction is only 1.0651, as shown in Table 2. The maximum value of  $Rot_{100}/Rot_{00}$  of the collapse load with the change of incident direction is only 1.1033, as shown in Table 3.

From the above analysis, it can be seen that the incident direction has a slight effect on the seismic response of SSRS, and the maximum difference in seismic response values under excitations with different incident angles does not exceed 10%. Additionally, the SSRS analyzed in this study is divided

into eight sections on average by radial members and each section has a spanning of 45°. According to the data in Figures 2–4, the seismic responses may vary with the incident angle in a periodic manner with a period of 45°, suggesting that the quantity of radial members in the SSRS is apparently correlated with the periodic variations in the structural seismic responses.

Table 1: *Rot100/Rot00* value of the vertical displacement.

PGA(g)	NGA No	IGD			
		<i>L</i> /1000	<i>L</i> /700	<i>L</i> /500	<i>L</i> /300
0.07	0006	1.0172	1.0146	1.0013	1.0091
	0015	1.0186	1.0171	1.0197	1.0069
	0138	1.0075	1.0025	1.0168	1.0128
	0704	1.0164	1.0157	1.0090	1.0046
	0945	1.0064	1.0320	1.0257	1.0077
	1181	1.0120	1.0185	1.0193	1.0122
	1762	1.0158	1.0183	1.0145	1.0148
0.2	0006	1.0291	1.0257	1.0087	1.0001
	0015	1.0314	1.0252	1.0370	1.0071
	0138	1.0064	1.0046	1.0363	1.0184
	0704	1.0309	1.0304	1.0175	1.0100
	0945	1.0082	1.0480	1.0368	1.0329
	1181	1.0122	1.0270	1.0266	1.0224
	1762	1.0249	1.0351	1.0246	1.0298
0.4	0006	1.0357	1.0328	1.0228	1.0082
	0015	1.0353	1.0346	1.0427	1.0075
	0138	1.0185	1.0125	1.0329	1.0126
	0704	1.0405	1.0406	1.0239	1.0148
	0945	1.0186	1.0362	1.0245	1.0651
	1181	1.0274	1.0241	1.0186	1.0099
	1762	1.0269	1.0325	1.0305	1.0289
0.6	0006	1.0172	1.0146	1.0013	1.0091
	0015	1.0186	1.0171	1.0197	1.0069
	0138	1.0075	1.0025	1.0168	1.0128
	0704	1.0164	1.0157	1.0090	1.0046
	0945	1.0064	1.0320	1.0257	1.0077
	1181	1.0120	1.0185	1.0193	1.0122
	1762	1.0158	1.0183	1.0145	1.0148

Table 2: Maximum value of *Rot100/Rot00* of the maximum collapse load.

NGA No	0006	0015	0138	0704	0945	1181	1762
<i>Rot100/Rot00</i>	1.0553	1.0994	1.0244	1.0426	1.1033	1.0947	1.0253

## 4.2 Half-span load on SSRS

In some force conditions, live loads on a structure such as snow loads may only occur over half of the structural area. The case of half-span loading may exacerbate the asymmetry of the structure, which may increase the impact of directionality on the seismic response of SSRS. Therefore, for a SSRS with an IGD of  $L/300$ , numerical analysis is conducted to determine its seismic response under ground motions (0.2g) with different incident directions. The live load of  $25 \text{ kg/m}^2$  is applied over half the span and at the most unfavorable location.

As shown in Table 4, the  $Rot100/Rot00$  values considering half-span load are much higher than those considering full-span load in Table 2, on average, 10% higher. It is significantly implied that the half-span load increases the structural asymmetry. From this analysis, it can be concluded that the effect of the incident angle on the seismic response of SSRS should be concerned when considering the combined action of half-span loading and IGD.

Table 4:  $Rot100/Rot00$  values of the vertical displacement.

NGA No	0006	0015	0138	0704	0945	1181	1762
$Rot100/Rot00$	1.1305	1.1688	1.0873	1.1237	1.0752	1.0937	1.1159

## 4.3 Arrangement of radial members on SSRS

The SSRS mentioned in the above analysis is divided into 8 sections by radial members along the radial direction, and each section has a spanning of  $45^\circ$ . To clarify the influence of the arrangement of radial members on the directional conclusions of seismic incidence, two finite element models of SSRS are established considering the IGD of  $L/300$ . Keeping other parameters constant, the number of radial members along the radial direction is changed to 4 and 6 respectively, and each section has a spanning of  $60^\circ$  and  $30^\circ$ , respectively. For the convenience of description, the above models are referred to as SSRS- $n$ , where  $n = 4, 6, \text{ and } 8$ .

According to Figure 5 and Figure 6, it can be seen that the period of the response of SSRS-4 is  $90^\circ$ , whereas that of SSRS-6 is  $60^\circ$ . The conclusion in Section 4.1 is that the period of the response of SSRS-6 is  $45^\circ$ . It is remarkably indicated that the periodicity of structural response under multi-directional excitations is influenced by the method of meridional partitioning for the SSRS (i.e., the value of  $n$ ), and the period is  $360^\circ/n$ .

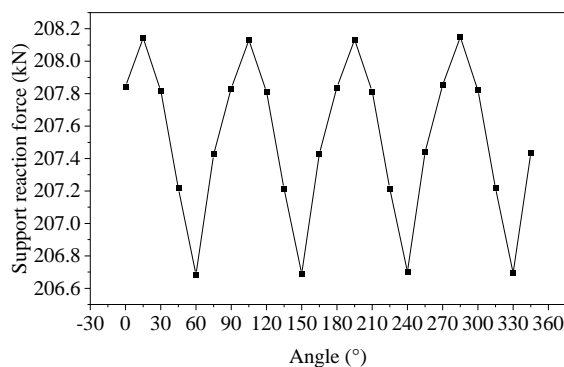


Figure 5: Support reaction forces of SSRS-4.

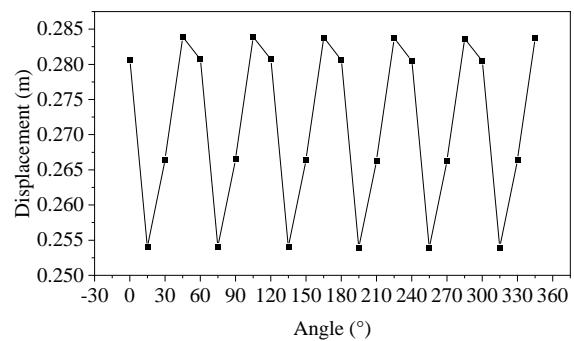


Figure 6: Vertical displacements of SSRS-8.

## 5. Conclusions

A numerical study is carried out to examine the influence of incident direction on the seismic responses of single-layer spherical reticulated shells with initial geometrical defects (SSRS-IGD) under 7 multi-dimensional ground motions with incident angles from  $0^\circ$  to  $360^\circ$ . The key findings are drawn as follows.

- (1) The incident direction has a slight impact on the seismic responses of SRSSs with different IGDs, the maximum  $Rot100/Rot00$  value of the vertical displacement is no more than 1.1.

(2) The effect of the incident angle on the seismic response of SSRS should be concerned when considering the combined action of half-span loading and IGD.

(3) The periodicity of structural response under multi-directional excitations is influenced by the method of meridional partitioning for the SSRS (i.e., the value of  $n$ ), and the period is  $360^\circ/n$ .

## References

- [1] J. Gong, X. Zhi, Y. Shao and Y. Luo, "State-of-the-art of research on seismic incident directionality effect of civil engineering structures," *Engineering Mechanics*, In press, 2024. (in Chinese)
- [2] Liang, W., Xia, L., Zhu, Z., Mou, S., Zou, Z. and Yuan, S.(2022), "Torsional effect of the single-bay masonry building considering seismic wave incident angle", *Structures*. 44, pp. 1232-1246.
- [3] Bugueño, I. , Carvallo, J. and Vielma, J. C. (2022), "Influence of Directionality on the Seismic Response of Typical RC Buildings", *Applied Sciences*. 12(3),1534.
- [4] Sun, M., Fan, F., Sun, B. and Zhi, X. (2016), "Study on the effect of ground motion direction on the response of engineering structure", *Earthquake Engineering and Engineering Vibration*. 15(4), pp. 649-656.
- [5] Alam, Z., Sun, L., Zhang, C. and Samali, B. (2022), "Influence of seismic orientation on the statistical distribution of nonlinear seismic response of the stiffness-eccentric structure", *Structures*. 39, pp. 387-404.
- [6] Torbol, M. and Shinozuka, M. (2012), "Effect of the angle of seismic incidence on the fragility curves of bridges", *Earthquake Engineering & Structural Dynamics*. 41(14), pp. 2111-2124.
- [7] Feng, R., Wang, X., Yuan, W. and Yu, J. (2018), "Impact of seismic excitation direction on the fragility analysis of horizontally curved concrete bridges", *Bulletin of Seismic Engineering*. 16(10), pp. 4705-4733.
- [8] Gong, J, Zhi, X. and Fan, F. (2021), "Effect of incident directionality on seismic responses and bearing capacity of OLF1000", *Engineering Structures*. 242,112542.
- [9] Li, W, "Research on the constitutive behavior of steel and the cumulative damage effect of grid shell structures based on the Xue-Wierzbicki damage criterion", master's thesis in *Harbin Institute of Technology*, 2016. (in chinese)
- [10] Ancheta, T. D., Darragh, R. B., Stewart, J. P., Seyhan, E., Silva, W. J. , Chiou, B. S-J, et al. (2014), "NGA West2 Database". *Earthquake Spectra*. 30(3), pp. 989-1005.
- [11] J. Gong, X. Zhi and F. Fan. "Effect of incident directionality on seismic responses and bearing capacity of OLF1000," *Engineering Structures*, vol. 242, no. 112542, pp. 1-13 2021.